https://doi.org/10.3311/PPtr.20076

Periodica Polytechnica Transportation Engineering, 50(4), pp. 309–317, 2022

Real-time Damper Force Estimation for Automotive Suspension

A Generalized H_2/LPV Approach

Thanh-Phong Pham[1*], Gia Quoc Bao Tran[2], Olivier Sename[2**], Thi Thanh Van Phan[1], Dung Hoang[1], Quoc Dinh Nguyen[3]

[1] Department of Automation, Faculty of Electrical and Electronic Engineering, University of Technology and Education – The University of Danang, 48 Cao Thang street, 550000 Danang, Vietnam
[2] GIPSA-lab, CNRS, Grenoble INP, Université Grenoble Alpes, 11 Rue des Mathématiques, 38402 Saint-Martin-d'Hères, France
[3] Department of Automation, Faculty of Electrical Engineering, University of Science and Technology – The University of Danang, 54 Nguyen Luong Bang street, 550000 Danang, Vietnam
[*] First corresponding author, e-mail: ptphong@ute.udn.vn
[**] Second corresponding author, e-mail: olivier.sename@gipsa-lab.grenoble-inp.fr

Received: 01 March 2022, Accepted: 29 June 2022, Published online: 02 August 2022

Abstract

The real-time knowledge of the damper force is of paramount importance in controlling and diagnosing automotive suspension systems. This study presents a generalized H_2/LPV observer for damper force estimation of a semi-active electro-rheological (ER) suspension system. First, an extended quarter-car model augmented with the nonlinear and dynamical model of the semi-active suspension system is written into the quasi-LPV formulation. Then, the damper force estimation method is developed through a generalized H_2/LPV observer whose objective is to handle the impact of unknown road disturbances and sensor noise on the estimation errors of the state variables thanks to the H_2 norm. The measured sprung and unsprung mass accelerations of the quarter-car system are used as inputs for the observer. The proposed approach is simulated with validated model of the 1/5-scaled real vehicle testbed of GIPSA-lab. Simulation results show the performance of the estimation method against unknown disturbances, emphasizing the effectiveness of the damper force estimation in real time.

Keywords

semi-active suspension, damper force estimation, generalized H_2/LPV observer, quasi-LPV

1 Introduction

Semi-active suspension systems remain an interesting research topic for both academia and industry thanks to their advantages, including lower weight and energy consumption compared to active and passive ones (see Savaresi et al., 2010). In their application, the real-time knowledge of damper (or damping) force plays a vital role in controlling (see Do et al. (2010); Nguyen et al. (2015); Poussot-Vassal et al. (2008; 2012) and Priyandoko et al. (2009)) and monitoring these systems (see Morato et al. (2019)). However, the direct measurement of this force using sensors faces some issues such as difficulty and expenses in installing and maintaining these sensors, leading to the increasing demand in adopting observers to estimate the damper force.

The main requirements of a damper force estimation approach include considering the dynamic characteristics of the semi-active damper and handling the nonlinearity and the unknown inputs in the dynamic model, as well as the use of the low-cost sensors (Pham, 2020). According to the considered dynamic behavior of the semi-active damper, the estimation methodologies are classified into two categories. In the first one, the parallel Kalman filters (Koch et al., 2010) and the data analysis methods (Savaresi et al., 2019) were developed to estimate the damper force, ignoring the dynamic characteristics of the semi-active damper. The second category is developed based on the dynamic damper models (Tudon-Martinez et al., 2018; Pham et al., 2019a; 2019b; 2019c;

Cite this article as: Pham, T.-P., Tran, G. Q. B., Sename, O., Phan, T. T. V., Hoang, D., Nguyen, Q. D. (2022) "Real-time Damper Force Estimation for Automotive Suspension: A Generalized H_2/LPV Approach", Periodica Polytechnica Transportation Engineering, 50(4), pp. 309–317. https://doi.org/10.3311/PPtr.20076

Vela et al., 2018). From the viewpoint of the required sensors, Tudon-Martinez et al. (2018) and Vela et al. (2018) presented a H_∞ observer and a linear parameter-varying (LPV) - H_∞ filter, respectively, for damper force estimation using the deflection and the deflection velocity as inputs. However, it is worth noting that deflection sensors are also costly and difficult to install in commercial cars. Therefore, based on accelerometers, some estimation approaches are developed by Koch et al. (2010) and Pham et al. (2019a; 2019b;2019c; 2021). On the other hand, to deal with the nonlinearity and unknown input disturbances in the dynamic model, many LMI-based methods are proposed in the literature, such as Tudon-Martinez et al. (2018); Pham et al. (2019a; 2019b; 2019c) and Vela et al. (2018). In particular, Tudon-Martinez et al. (2018) wrote the dynamic system into the LPV form with the nonlinearity considered as a scheduling variable and then used the sensors to compute the scheduling parameter, leading to an increase in the required input sensors.

To deal with the above issues, the authors have developed several estimation approaches using a nonlinear dynamic model of the semi-active damper and the two accelerometers, while the nonlinearity is bounded by a Lipschitz condition. Using two accelerometers, Pham et al. (2019a; 2019b) developed two damper force estimation methods based on the H_∞ and unified H_∞ observers, respectively. In these studies, the nonlinearity in the electro-rheological (ER) damper model is bounded by the Lipschitz condition. However, the results from the above nonlinear Lipschitz modeling can be conservative due to the presence of the maximum control bound in the LMI. To relax the conservatism, the dynamic system is modeled into the nonlinear parameter-varying (NLPV) representation, and an NLPV observer is then proposed to estimate the damper force by using the H_∞ criterion to minimize the effect of unknown disturbances on the estimation error (Pham et al., 2019c; 2021).

In this work, the extended quarter-car model is represented in a quasi-LPV form, where the nonlinearity in the ER damper model is defined as the scheduling parameter. Then, a generalized H_2/LPV observer is proposed to estimate the damping force in the presence of unknown road input and measurement noise, while the scheduling variable is obtained from estimated states. The error between the estimated scheduling variable and the real one is considered as an unknown input, which is handled using the generalized H_2 norm. The contributions of this paper are then summarized as:

- A generalized H_2/LPV observer is developed to estimate the damper force, minimizing the effect of unknown disturbances on the estimation error w.r.t the energy-to-peak gain.
- The proposed approach is simulated with a validated model of the 1/5-scaled testbed at GIPSA-lab (ANR, 2010). The simulation results demonstrate the effectiveness of the method.

The rest of the paper is organized as follows. Firstly, the quarter-car system modeling is presented in Section 2. The central part of this paper, observer formulation and design method, is detailed in Section 3. In Section 4, the observer is synthesized and analyzed in the frequency domain. To demonstrate the effectiveness of the observer, simulation results are given in Section 5. Finally, the concluding remarks are presented in Section 6.

2 Quarter-car system modeling

2.1 Physical model

Section 2.1 shows the quarter-car model augmented with the semi-active ER suspension system depicted in Fig. 1. The dynamic model includes the sprung mass (m_s), the unsprung mass (m_{us}), the semi-active suspension located between (m_s) and (m_{us}), and the tire, which is modeled as a spring with stiffness k_t. From Newton's second law of motion, the system dynamics around the equilibrium are given as follows:

$$\begin{cases} m_s \ddot{z}_s = -F_s - F_d \\ m_{us}\ddot{z}_{us} = F_s + F_d - F_t \end{cases}, \tag{1}$$

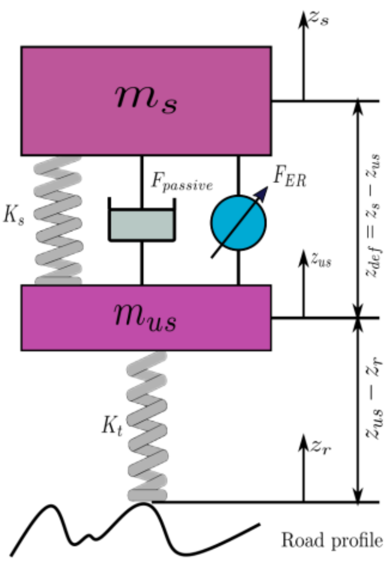

Fig. 1 1/4 car model with semi-active suspension

where $F_s = k_s(z_s - z_{us})$ is the spring force; $F_t = k_t(z_{us} - z_r)$ is the tire force; the damper force F_d is later presented in Eq. (2); z_s and z_{us} are the displacements of the sprung and unsprung masses, respectively; z_r is the road displacement input.

From Pham (2020), the nonlinear dynamical model of semi-active ER damper is given as

$$\begin{cases} F_d = k_0\left(z_s - z_{us}\right) + c_0\left(\dot{z}_s - \dot{z}_{us}\right) + F_{er} \\ \dot{F}_{er} = -\dfrac{1}{\tau}F_{er} + \dfrac{f_c}{\tau}\cdot u \cdot \tanh\left(k_1\left(z_s - z_{us}\right) + c_1\left(\dot{z}_s - \dot{z}_{us}\right)\right) \end{cases}, \quad (2)$$

where F_d is the damper force; c_0, c_1, k_0, k_1, f_c, and τ are constant parameters. The parameters of the model in Eq. (2) are shown in Table 1. The control input u is the applied voltage that provides the electrical field to control the ER damper. In practice, it is the duty cycle of the PWM signal that controls the application (shown in Table 2).

2.2 Quasi-LPV modeling

By selecting the system states as $x = \left[x_1, x_2, x_3, x_4, x_5\right]^T = \left[z_s - z_{us}, \dot{z}_s, z_{us} - z_r, \dot{z}_{us}, F_{er}\right]^T \in \mathbb{R}^5$, the measured variables $y = \left[\ddot{z}_s, \ddot{z}_{us}\right]^T \in \mathbb{R}^2$, choosing now the scheduling parameters $\rho_1 = \tanh\left(k_1\left(z_s - z_{us}\right) + c_1\left(\dot{z}_s - \dot{z}_{us}\right)\right) \in \mathbb{R}$, $\rho_2 = u$, the system dynamics can be formulated into the following quasi-LPV representation

$$\begin{cases} \dot{x} = \boldsymbol{A}x + \boldsymbol{B}\left(\rho_1\right)\cdot\rho_2 + \boldsymbol{D}_1\omega \\ y = \boldsymbol{C}x + \boldsymbol{D}_2\omega \end{cases}, \quad (3)$$

Table 1 Parameters of the quarter-car model with an ER damper

Parameter	Description	Value	Unit
m_s	Sprung mass	2.27	kg
m_{us}	Unsprung mass	0.25	kg
k_s	Spring stiffness	1396	N/m
k_t	Tire stiffness	12270	N/m
k_0	Effective stiffness coefficient due to the gas pressure	170.4	N/m
c_0	Viscous damping coefficient in the absence of control input	68.83	N s/m
k_1	Hysteresis coefficient due to displacement	218.16	N s/m
c_1	Hysteresis coefficient due to velocity	21	N s/m
f_c	Dynamic yield force of ER fluid	28.07	N
τ	Time constant	43	ms

Table 2 Range of the control input value u

Control input	Description	Value
u	Duty cycle of PWM channel	[0, 1]

where $\omega = \begin{pmatrix} \omega_r \\ n_y \end{pmatrix}$, in which $\omega_r = \dot{z}_r$ is the road profile derivative and n_y is the sensor noises, and the system matrices are as follows:

$$\boldsymbol{A} = \begin{bmatrix} 0 & 1 & 0 & -1 & 0 \\ \dfrac{-\left(k_s + k_0\right)}{m_s} & \dfrac{-c_0}{m_s} & 0 & \dfrac{c_0}{m_s} & \dfrac{-1}{m_s} \\ 0 & 0 & 0 & 1 & 0 \\ \dfrac{\left(k_s + k_0\right)}{m_{us}} & \dfrac{-c_0}{m_{us}} & \dfrac{-k_t}{m_{us}} & \dfrac{c_0}{m_{us}} & \dfrac{-1}{m_{us}} \\ 0 & 0 & 0 & 0 & \dfrac{-1}{\tau} \end{bmatrix},$$

$$\boldsymbol{B}\left(\rho_1\right) = \begin{bmatrix} 0 \\ 0 \\ 0 \\ 0 \\ \dfrac{fc}{\tau}\rho_1 \end{bmatrix},$$

$$\boldsymbol{C} = \begin{bmatrix} \dfrac{-\left(k_s + k_0\right)}{m_s} & \dfrac{-c_0}{m_s} & 0 & \dfrac{c_0}{m_s} & \dfrac{-1}{m_s} \\ \dfrac{\left(k_s + k_0\right)}{m_{us}} & \dfrac{-c_0}{m_{us}} & \dfrac{-k_t}{m_{us}} & \dfrac{c_0}{m_{us}} & \dfrac{-1}{m_{us}} \end{bmatrix},$$

$$\boldsymbol{D}_1 = \begin{bmatrix} 0 & 0 \\ 0 & 0 \\ -1 & 0 \\ 0 & 0 \\ 0 & 0 \end{bmatrix}, \ \boldsymbol{D}_2 = \begin{bmatrix} 0 & 0.01 \\ 0 & 0.01 \end{bmatrix}.$$

3 Observer design

3.1 Quasi-LPV observer definition

In Section 3.1, a generalized H_2/LPV observer is designed to estimate the damper force accurately.

According to the damper model in Eq. (2), the estimated force $\hat{F}_d$ can then be obtained as

$$\hat{F}_d = k_0\hat{x}_1 + c_0\left(\hat{x}_2 - \hat{x}_4\right) + \hat{x}_5 \ . \quad (4)$$

Therefore, the variables to be estimated are defined by the output vector $z = [x_1, x_2, x_3, x_4, x_5]^T$.

Finally, the generalized H_2//LPV observer for the system in Eq. (3) is formulated as

$$\begin{cases} \dot{\hat{x}} = \boldsymbol{A}\hat{x} + \boldsymbol{B}\left(\hat{\rho}_1\right)\cdot\rho_2 + \boldsymbol{L}\left(\rho_2\right)\left(y - \boldsymbol{C}\hat{x}\right) \\ \hat{z} = \boldsymbol{C}_z\hat{x} \end{cases}, \quad (5)$$

where $\hat{x}$ denotes the estimated states of the system's states x, $\hat{z}$ denotes the estimated variables of z. The observer gain $\boldsymbol{L}(\rho_2)$ is to be obtained through an optimization problem that is detailed in Section 3.2 (in the framework of quadratic stability of the estimation error).

3.2 Observer design

The state estimation error $e(t)$ is defined as

$$e(t) = x(t) - \hat{x}(t). \tag{6}$$

Differentiating $e(t)$ w.r.t time and using Eq. (3) and Eq. (6), one obtains

$$\begin{cases} \dot{e} = \dot{x} - \dot{\hat{x}} = \boldsymbol{A}x + \boldsymbol{B}(\rho_1)\cdot\rho_2 + \boldsymbol{D}_1\omega \\ -\boldsymbol{A}\hat{x} - \boldsymbol{L}(\rho_2)(y - \boldsymbol{C}\hat{x}) - \boldsymbol{B}(\hat{\rho}_1)\cdot\rho_2 \\ e_z = \boldsymbol{C}_z e \end{cases}, \tag{7}$$

equivalently,

$$\begin{cases} \dot{e} = (\boldsymbol{A} - L(\rho_2)\boldsymbol{C})e + (\boldsymbol{B}(\rho_1) - \boldsymbol{B}(\hat{\rho}_1))\cdot\rho_2 \\ +(\boldsymbol{D}_1 - L(\rho_2)\boldsymbol{D}_2)\omega \\ e_z = \boldsymbol{C}_z e \end{cases}. \tag{8}$$

In this work $\boldsymbol{B}(\rho_1) - \boldsymbol{B}(\hat{\rho}_1)$ is the inexact varying variable, which is considered as uncertainty. From the system matrix $\boldsymbol{B}(\rho)$, one obtains

$$\boldsymbol{B}(\rho_1) - \boldsymbol{B}(\hat{\rho}_1) = \boldsymbol{B}\cdot(\rho_1 - \hat{\rho}_1), \tag{9}$$

where $\boldsymbol{B} = \begin{bmatrix} 0 & 0 & 0 & 0 & f_c/\tau \end{bmatrix}^T$. Here, we assume that this uncertainty $(\rho_1 - \hat{\rho}_1)$ is bounded by a constant as

$$(\rho_1 - \hat{\rho}_1) = \Delta\boldsymbol{\rho}_1 \cdot n_\rho, \tag{10}$$

where $\Delta\boldsymbol{\rho}_1$ is a constant matrix and n_ρ is white noise. Denoting $\Delta\boldsymbol{B} = \boldsymbol{B}\Delta\boldsymbol{\rho}_1$, the dynamic estimation error system in Eq. (8) is written as

$$\begin{cases} \dot{e} = (\boldsymbol{A} - L(\rho_2)\boldsymbol{C})e + \Delta\boldsymbol{B}(\rho_2)\cdot n_\rho + (\boldsymbol{D}_1 - L(\rho_2)\boldsymbol{D}_2)\omega \\ e_z = \boldsymbol{C}_z e \end{cases}. \tag{11}$$

Defining a new unknown input $\omega_n = \begin{pmatrix} n_\rho \\ \omega \end{pmatrix}$, Eq. (11) is rewritten as

$$\begin{cases} \dot{e} = (\boldsymbol{A} - L(\rho_2)\boldsymbol{C})e + \boldsymbol{D}(\rho_2)\omega_n \\ e_z = \boldsymbol{C}_z e \end{cases}, \tag{12}$$

where $\boldsymbol{D}(\rho_2) = \left[\Delta\boldsymbol{B}(\rho_2)(\boldsymbol{D}_1 - L(\rho_2)\boldsymbol{D}_2)\right]$.

Since the system in Eq. (12) only depends on ρ_2 we can choose to define the observer gain $\boldsymbol{L}(\rho_2)$ in a polytopic form as $\boldsymbol{L}(\rho_2) = \sum_{i=1}^{2}\alpha_i(\rho_2)\boldsymbol{L}_i$, where $\boldsymbol{L}_i$ is the observer gain at each vertex of ρ_2 and $\sum_{i=1}^{2}\alpha_i(\rho_2) = 1$.

The generalized H_2/LPV observer design objectives are:

- the system in Eq. (12) is stable for $\omega_n = 0$;
- $\dfrac{\|e_z\|_\infty}{\|\omega_n\|_2}$ is minimized for $\omega_n \neq 0$.

The following theorem solves the above problem following an LMI framework (Scherer and Weiland, 2015).

Theorem 1: *Consider the system model in Eq. (3) and the observer in Eq. (5). If there exists a symmetric positive definite matrix* $\boldsymbol{P}$ *and matrices* $\boldsymbol{Y}_i$ *with* $i = 1, 2$ *minimizing* γ *such that*

$$\begin{pmatrix} \boldsymbol{PA} + \boldsymbol{A}^T\boldsymbol{P} - \boldsymbol{Y}_i\boldsymbol{C} - (\boldsymbol{Y}_i\boldsymbol{C})^T & \boldsymbol{P}\Delta\boldsymbol{B}(\rho_{2i}) & \boldsymbol{PD}_1 - \boldsymbol{Y}_i\boldsymbol{D}_2 \\ \Delta\boldsymbol{B}(\rho_{2i})^T\boldsymbol{P} & -\boldsymbol{I} & 0 \\ \boldsymbol{D}_1^T\boldsymbol{P} + (\boldsymbol{YD}_2)^T & 0 & -\boldsymbol{I} \end{pmatrix} < 0,$$
$$\begin{pmatrix} \boldsymbol{P} & \boldsymbol{C}_z^T \\ \boldsymbol{C}_z & \gamma\boldsymbol{I} \end{pmatrix} > 0, \tag{13}$$

then the observer vertex matrices $\boldsymbol{L}_i$ *determined from* $\boldsymbol{L}_i = \boldsymbol{P}^{-1}\boldsymbol{Y}_i$ *ensure that the objectives are attained.* $\boldsymbol{I}$ *is the identity matrix.*

Proof. The proof is not detailed here since it consists in a simple application of the generalized H_2 condition to each vertex of the dynamic estimation error system in Eq. (12).

4 Observer synthesis and frequency domain analysis

4.1 Observer synthesis

As previously mentioned, the scheduling variable $\rho_1 = \tanh(k_1x_1 + c_1(x_2 - x_4))$ is limited in the range of [−1, 1] and $\rho_2 = u$ varies in the range of [0, 1]. Therefore, the following values are obtained:

- the lower bound of ρ_2 is $\underline{\rho}_2 = 0$;
- the upper bound of ρ_2 is $\overline{\rho}_2 = 1$.

The Yalmip toolbox (Lofberg, 2004) and the sdpt3 solver (Toh et al., 1999) are used to solve the optimization in Theorem 1. Solving Theorem 1 with the two above vertices leads to the minimum $\boldsymbol{L}_2$-induced gain $\gamma = 0.478$, and to the observer vertex matrices

$$\boldsymbol{L}_1 = \begin{bmatrix} -0.1011 & 0 \\ -0.0093 & -0.0002 \\ 32.7307 & -327.9806 \\ -0.1009 & 1 \\ -128.9226 & -0.3546 \end{bmatrix},$$

$$\boldsymbol{L}_2 = \begin{bmatrix} -0.0998 & 0.0002 \\ 0.0018 & 0.0014 \\ 32.7413 & -327.9807 \\ -0.0998 & 0.2794 \\ -128.0171 & \end{bmatrix}.$$

4.2 Frequency-domain analysis

In Section 4.2, the analysis of the effects of unknown inputs (road profile derivative ω_r and measurement noises n) on the estimation error e in the frequency domain is performed using the Bode diagrams.

The transfer functions from ω_r and n to the estimation error e_z are shown on the left and right sides of Fig. 2. As shown, the Bode diagrams of the polytopic at the frozen values of two vertices ($\underline{\rho}_2 = 0$ (red line) and $\overline{\rho}_2 = 1$ (green dash-dot dot)) emphasizes the satisfactory attenuation level of the unknown disturbances on the estimation error.

5 Simulation results

In Section 5, simulations with different scenarios are performed to validate the designed observer in the time domain.

5.1 Simulation scenario 1

This simulation scenario is as follows:

- The road profile input is a chirp signal with an amplitude of 7×10^{-3} m and various frequencies from 0 Hz to 10 Hz (shown in Fig. 3).
- The scheduling parameter ρ_2 ($\rho_2 = u$) is obtained from a Skyhook controller (see Fig. 4).

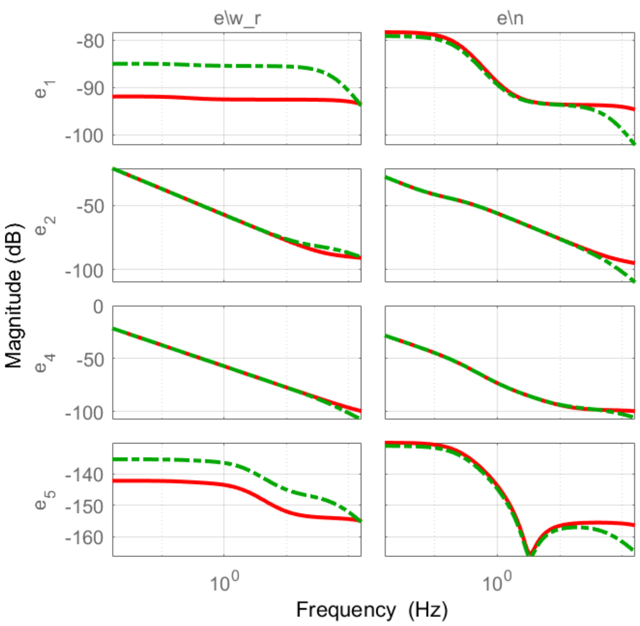

Fig. 2 Bode diagram w.r.t road profile derivative (left) and measurement noise (right)

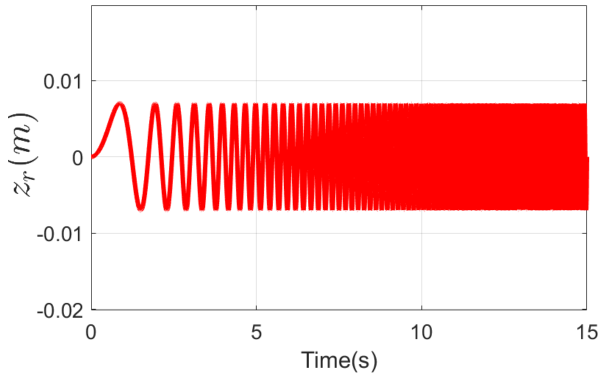

Fig. 3 Simulation scenario 1: Road profile

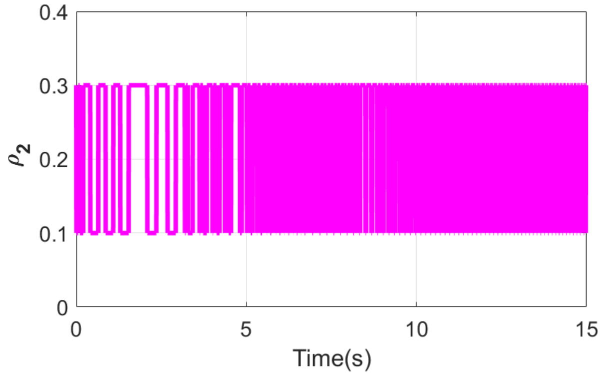

Fig. 4 Simulation scenario 1: Scheduling parameter ρ_2

The estimated scheduling variable $\hat{\rho}_1$ is shown in Fig. 5. Fig. 6 shows the simulated force in the solid red line and the estimated force in the blue dotted line, respectively. The estimation error is shown in Fig. 7. We can see that the estimation error converges to 0 after 1 second. Therefore, the proposed method is stable with the various frequencies of road profile disturbance.

5.2 Simulation scenario 2

In the second simulation scenario, the proposed observer is validated with more realistic road profile.

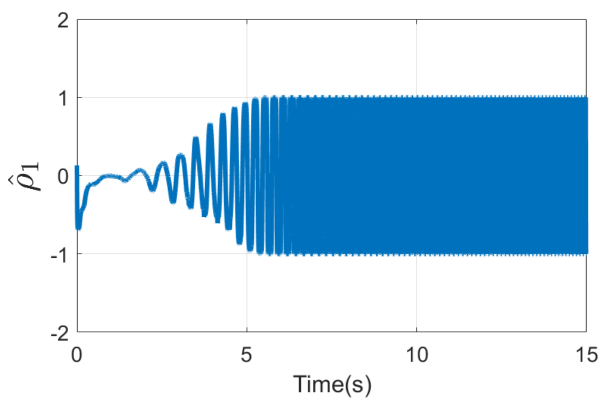

Fig. 5 Simulation scenario 1: Estimated scheduling parameter $\hat{\rho}_1$

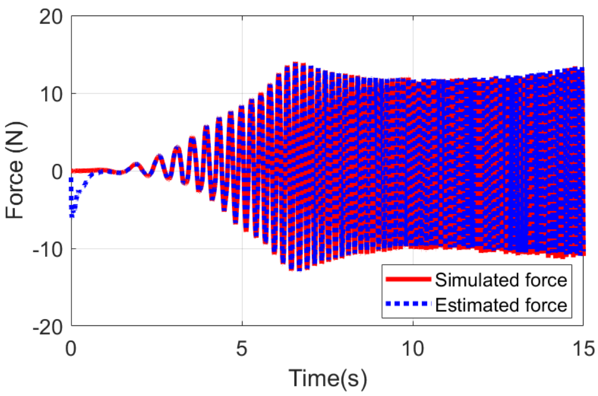

Fig. 6 Simulation scenario 1: Real and estimated damper force

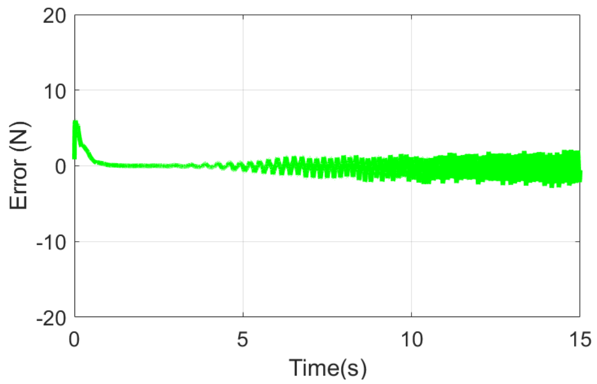

Fig. 7 Simulation scenario 1: Estimation error

The second simulation is designed as follows:

- A realistic road profile (ISO type C) is used (shown in Fig. 8).
- The scheduling parameter ρ_2 ($\rho_2 = u$) comes from a Skyhook controller (shown in Fig. 9).

The estimated scheduling parameter $\hat{\rho}_1$ is shown in Fig. 10. The simulation results of this scenario are shown in Figs. 11 and 12. The results show the stability of the proposed schemes $e \rightarrow 0$ in a realistic case. It is worth noting that the observer must work when the sensors are affected

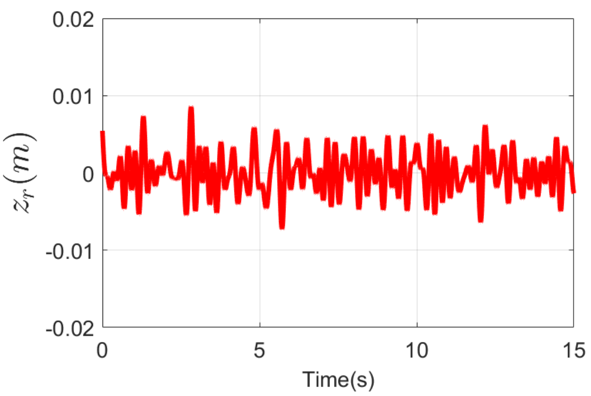

Fig. 8 Simulation scenario 2: ISO road profile (Type C)

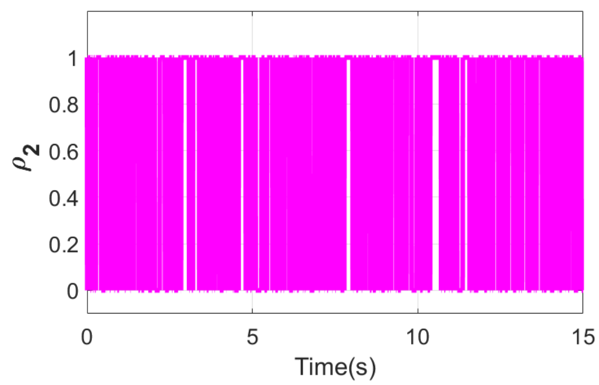

Fig. 9 Simulation scenario 2: Scheduling parameter ρ_2

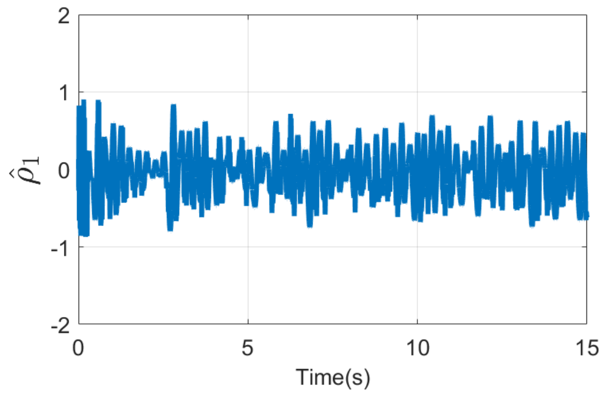

Fig. 10 Simulation scenario 2: Estimated scheduling parameter $\hat{\rho}_1$

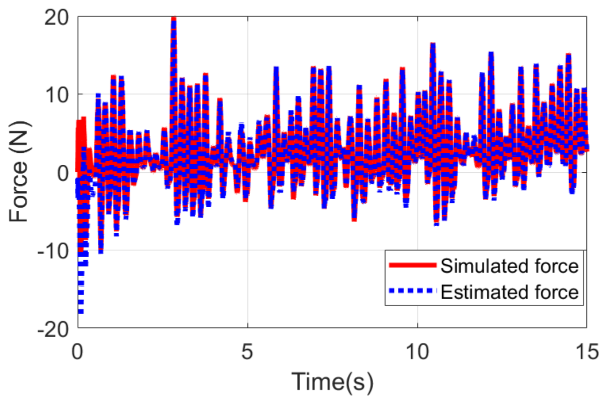

Fig. 11 Simulation scenario 2: Real and estimated damper force

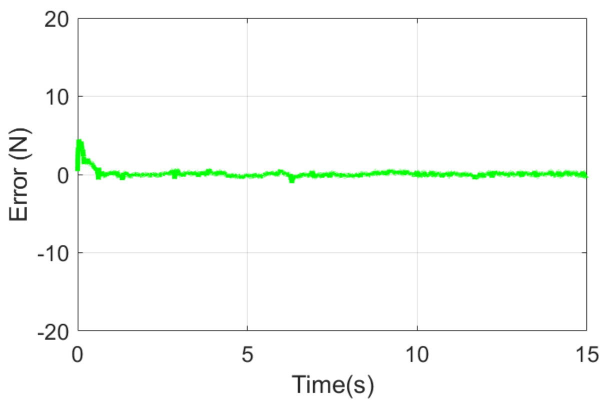

Fig. 12 Simulation scenario 2: Estimation error

by noises in the real application. Therefore, to assess the effectiveness of the observer affected by noises, a more realistic scenario is presented in Section 5.3.

5.3 Simulation scenario 3

This scenario is designed by adding the noises into the measurement outputs, detailed as follows:

- A sinusoidal road profile is considered in this scenario (shown in Fig. 13).
- The scheduling parameter ρ_2 is obtained from a Skyhook controller (Fig. 14).
- The sensors are affected by noises (shown in Figs. 15 and 16).

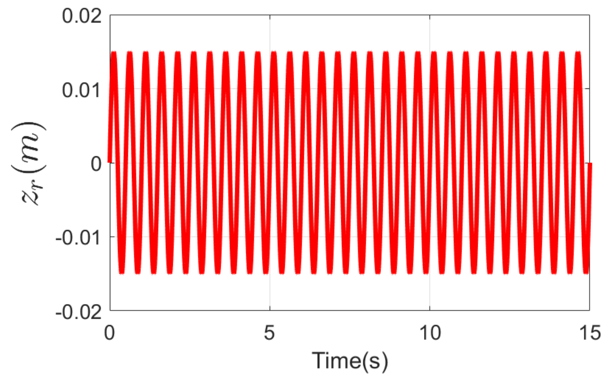

Fig. 13 Simulation scenario 3: road profile

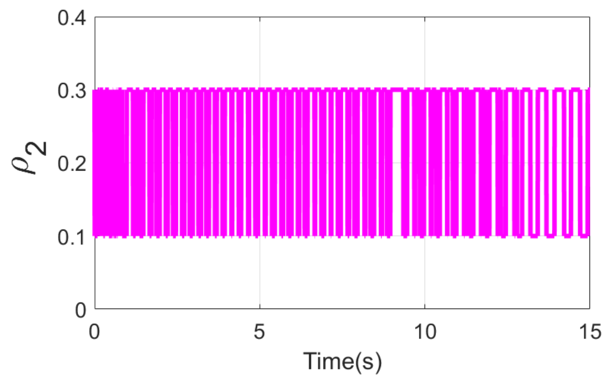

Fig. 14 Simulation scenario 3: Scheduling parameter ρ_2

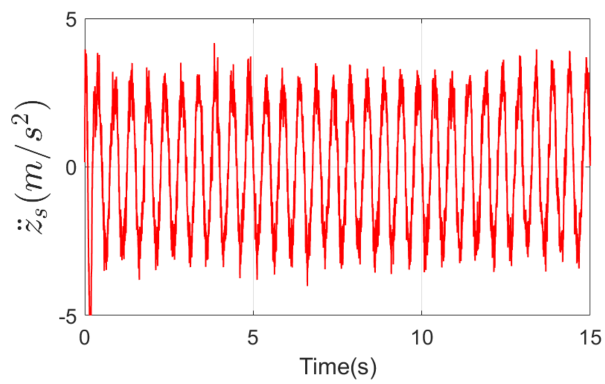

Fig. 15 Simulation scenario 3: Sprung mass acceleration affected by noise

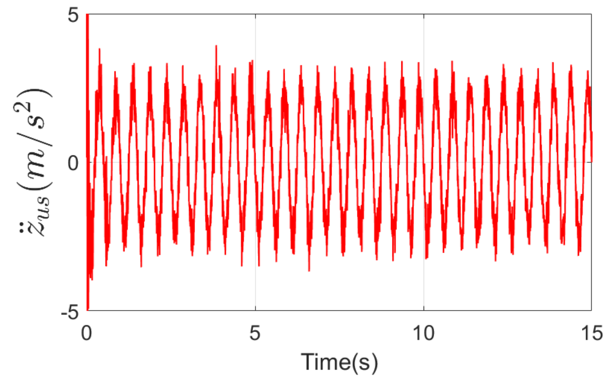

Fig. 16 Simulation scenario 3: Unsprung mass acceleration affected by noise

The estimated scheduling parameter $\hat{\rho}_1$ is presented in Fig. 17. The damper estimation results of this scenario are shown in Fig. 18 while the estimation error is seen in Fig. 19. The results present the robustness of the proposed approaches in the presence of the sensor noises.

6 Conclusion

This paper presents a generalized H_2/LPV observer to estimate the damper force. For this purpose, the quarter-car system is formulated in a quasi-LPV form. A generalized H_2/LPV observer using accelerometer measurements as input is developed, providing an accurate estimation of

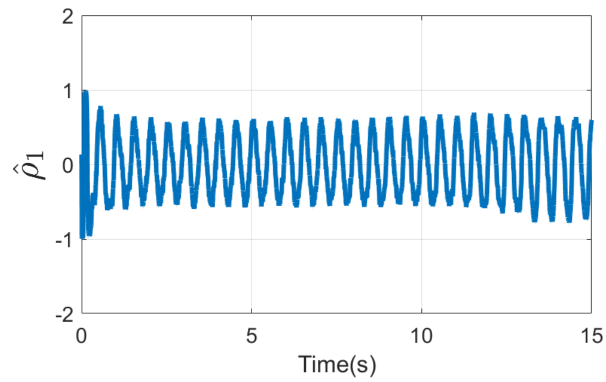

Fig. 17 Simulation scenario 3: Estimated scheduling parameter $\hat{\rho}_1$

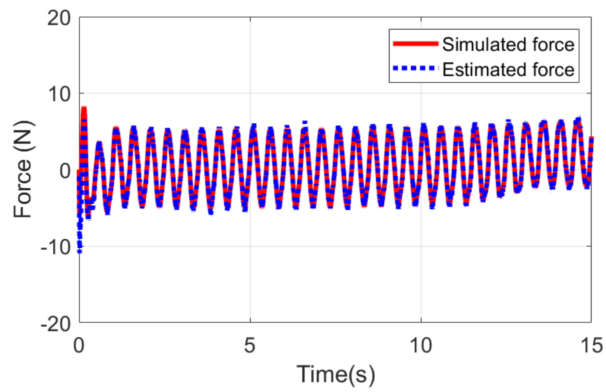

Fig. 18 Simulation scenario 3: damper force

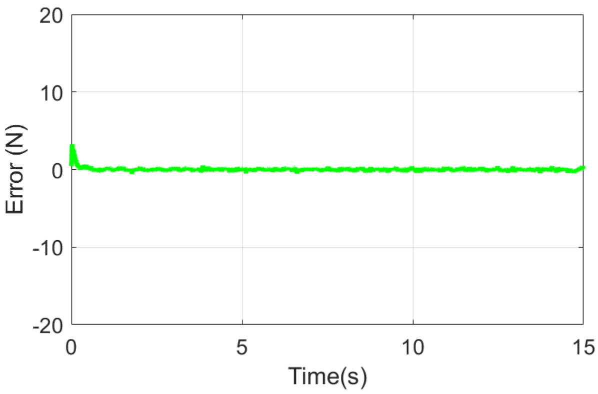

Fig. 19 Simulation scenario 3: Estimation error

the damper force in real-time. The force estimation error is minimized, accounting for the effect of unknown inputs (road profile derivative measurement noise). The simulation results show the performance and the accuracy of the proposed approach.

Acknowledgement

This research work has been supported by the PHC BALATON project under project number 41854PM.

References

ANR (2010) "INOVE", [online] Available at: http://www.gipsa-lab.fr/projet/inove/index.html [Accessed: 10 December 2021]

Do, A.-L., Sename, O., Dugard, L. (2010) "An LPV Control Approach for Semi-active Suspension Control with Actuator Constraints", In: Proceedings of the 2010 American Control Conference, IEEE, pp. 4653–4658. ISBN 978-1-4244-7426-4 https://doi.org/10.1109/ACC.2010.5531069

Koch, G., Kloiber, T., Lohmann, B. (2010) "Nonlinear and Filter Based Estimation for Vehicle Suspension Control", In: 49th IEEE Conference on Decision and Control (CDC), IEEE, pp. 5592–5597. ISBN 978-1-4244-7745-6 https://doi.org/10.1109/CDC.2010.5718052

Lofberg, J. (2004) "YALMIP: A Toolbox for Modeling and Optimization in MATLAB", In: 2004 IEEE International Conference on Robotics and Automation, IEEE, pp. 284–289. ISBN 0-7803-8636-1 https://doi.org/10.1109/CACSD.2004.1393890

Morato, M. M., Sename, O., Dugard, L., Nguyen, M. Q. (2019) "Fault Estimation for Automotive Electro-Rheological Dampers: *LPV*-based Observer Approach", Control Engineering Practice, 85, pp. 11–22. https://doi.org/10.1016/j.conengprac.2019.01.005

Nguyen, M. Q., Gomes da Silva, J. M., Sename, O., Dugard, L. (2015) "Semi-active Suspension Control Problem: Some New Results Using an LPV/H_∞ State Feedback Input Constrained Control", In: 2015 54th IEEE Conference on Decision and Control (CDC), IEEE, pp. 863–868. ISBN 978-1-4799-7886-1 https://doi.org/10.1109/CDC.2015.7402337

Pham, T.-P. (2020) "LPV Observer and Fault-tolerant Control of Vehicle Dynamics: Application to an Automotive Semi-active Suspension System", Doctoral Dissertation, Université Grenoble Alpes.

Pham, T.-P., Sename, O., Dugard, L. (2019a) "Design and Experimental Validation of an H_∞ Observer for Vehicle Damper Force Estimation", IFAC-PapersOnLine, 52(5), pp. 673–678. https://doi.org/10.1016/j.ifacol.2019.09.107

Pham, T.-P., Sename, O., Dugard L. (2019b) "Unified H_∞ Observer for a Class of Nonlinear Lipschitz Systems: Application to a Real ER Automotive Suspension", IEEE Control Systems Letters, 3(4), pp. 817–822. https://doi.org/10.1109/LCSYS.2019.2919813

Pham, T.-P., Sename, O., Dugard, L. (2019c) "Real-time Damper Force Estimation of Vehicle Electrorheological Suspension: A NonLinear Parameter Varying Approach", IFAC-PapersOnLine, 52(28), pp. 94–99. https://doi.org/10.1016/j.ifacol.2019.12.354

Pham, T.-P., Sename, O., Dugard, L. (2021) "A nonlinear parameter varying observer for real-time damper force estimation of an automotive electro-rheological suspension system", International Journal of Robust and Nonlinear Control 2021, 31(17), pp. 8183–8205. https://doi.org/10.1002/rnc.5583

Poussot-Vassal, C., Sename, O., Dugard, L., Gaspar, P., Szabó, Z., Bokor, J. (2008) "A New Semi-active Suspension Control Strategy through LPV Technique", Control Engineering Practice, 16(12), pp. 1519–1534. https://doi.org/10.1016/j.conengprac.2008.05.002

Poussot-Vassal, C., Spelta, C., Sename, O., Savaresi, S. M., Dugard, L. (2012) "Survey and Performance Evaluation on Some Automotive Semi-active Suspension Control Methods: A Comparative Study on a Single-corner Model", Annual Reviews in Control, 36(1), pp. 148–160. https://doi.org/10.1016/j.arcontrol.2012.03.011

Priyandoko, G., Mailah, M., Jamaluddin, H. (2009) "Vehicle Active Suspension System using Skyhook Adaptive Neuro Active Force Control", Mechanical Systems and Signal Processing, 23(3), pp. 855–868. https://doi.org/10.1016/j.ymssp.2008.07.014

Savaresi, S. M., Poussot-Vassal, C., Spelta, C., Sename, O., Dugard, L. (2010) "Semi-active Suspension Control Design for Vehicles", Elsevier. ISBN 9780080966793

Savaresi, D., Favalli, F., Formentin, S., Savaresi, S. M. (2019) "On-line Damping Estimation in Road Vehicle Semi-active Suspension Systems", In: IFAC-PapersOnLine, 52(5), pp. 679–684. https://doi.org/10.1016/j.ifacol.2019.09.108

Scherer, C., Weiland, S. (2015) "Linear Matrix Inequalities in Control", [pdf] University of Stuttgart, Stuttgart, Germany. Available at: https://www.imng.uni-stuttgart.de/mst/files/LectureNotes.pdf [Accessed: 10 December 2021]

Toh, K. C., Todd, M. J., Tütüncü, R. H. (1999) "SDPT3 — A Matlab Software Package for Semidefinite Programming, Version 1.3", Optimization Methods and Software, 11(1–4), pp. 545–581. https://doi.org/10.1080/10556789908805762

Tudon-Martinez, J. C., Hernandez-Alcantara, D., Sename, O., Morales-Menendez, R., De J. Lozoya-Santos, J. de J. (2018) "Parameter-dependent H_∞ Filter for LPV Semi-active Suspension Systems", IFAC-PapersOnLine, 51(26), pp. 19–24. https://doi.org/10.1016/j.ifacol.2018.11.174

Vela, A. E., Alcántara, D. H., Menendez, R. M., Sename, O., Dugard, L. (2018) "H_∞ Observer for Damper Force in a Semi-active Suspension", IFAC-PapersOnLine, 51(11), pp. 764–769. https://doi.org/10.1016/j.ifacol.2018.08.411